

Design and fabrication of computer-generated holograms for testing optical freeform surfaces

Hua Shen (沈 华)^{1,2}, Rihong Zhu (朱日宏)^{1*}, Zhishan Gao (高志山)¹,
E. Y. B. PUN², W. H. Wong², and Xiaoli Zhu (朱效立)³

¹*School of Electronic Engineering and Photo-Electric Technology, Nanjing University of Science and Technology, Nanjing 210094, China*

²*Department of Electronic Engineering, City University of Hong Kong, Kowloon Tang, Hong Kong 999077, China*

³*Key Laboratory of Nano-Fabrication and Novel Devices Integrated Technology, Institute of Microelectronics of Chinese Academy of Sciences, Beijing 100029, China*

*Corresponding author: zhurihong@mail.njust.edu.cn

Received October 23, 2012; accepted November 5, 2012; posted online February 6, 2013

Freeform optical surfaces (FOSs) will be the best elements in the design of compact optical systems in the future. However, it is extremely difficult to measure freeform surface with sufficient accuracy, which impedes the development of the freeform surface. The design and fabrication of computer-generated hologram (CGH), which has been successfully applied to the tests for aspheric surfaces, cannot be directly adopted to test FOSs due to their non-rotational asymmetry. A novel ray tracing planning method combined with successively optimizing even and odd power coefficients of phase polynomials in turn is proposed, which can successfully design a non-rotational asymmetry CGH for the tests of FOSs with an F - θ lens. A new eight-step fabrication process is also presented aiming to solve the problem that the linewidth on the same circle of the CGH for testing freeform surface is not uniform. This problem cannot be solved in the original procedure of CGH fabrication. The test results of the step profiler show that the CGH fabricated in the new procedure meets the requirements.

OCIS codes: 220.1250, 050.1970, 090.1760, 220.4840.

doi: 10.3788/COL201311.032201.

Original optical systems composed by spherical and aspheric surfaces cannot satisfy the increasing demands for compactness and high quality with the development of the photo-electric technology. Freeform optical elements are widely used in many optoelectronic systems because they can correct several image aberrations effectively and simplify optical system structures^[1,2]. It has attracted considerable attention to design and fabricate several freeform surfaces^[3,4]. But the fabrication costs are too high and the quality of the freeform surfaces are not as good as aspheric surfaces because it is extremely difficult to accurately measure the quality of the freeform surfaces, which has been the focus in the optical measurement field^[5,6].

The interferometric method with computer generated hologram (CGH) is successfully applied to the precise testing of aspheric surfaces because CGH can provide arbitrary shape wavefront that compensates the departure of the tested surface from a spherical one in null test^[7-12]. Using CGH as a null corrector in the tests of freeform surfaces is feasible and valid because the freeform surfaces can be regarded as non-rotational asymmetry aspheric surfaces^[13]. However, when CGH is adopted to test freeform surfaces, the design, fabrication and alignment of CGH have been facing technical barriers caused by free shape, rapid gradient change, and definition difficulty of freeform surfaces. Until now, there are few reports on fabrication of non-rotational asymmetry CGH, and some of them focused on the design of non-rotational asymmetry CGH^[14,15] using cubic B-spline interpolation. A novel design method based on orthogonal basis set and fabrication process of CGH used

in tests of freeform surface with an F - θ lens is presented below.

When CGH is used for testing aspheric surfaces, according to the aplanatic principle, all optical paths from F' to the tested surface are equal, as shown in Fig. 1^[14]. Supposing the ray going through the point G_0 on the surface is the reference ray and considering an arbitrary ray launches onto G on the tested surface along the corresponding normal direction, the optical path difference is

$$w(x_s, y_s, z_s) = |F'E| + n_2 |ET| + |TG| - |FF'| - n_2 |FR| - |RG_0|, \quad (1)$$

where n_2 is the refractive index of the substrate of the CGH. $|F'E|$, $|ET|$, $|TG|$, $|FF'|$, $|FR|$, and $|RG_0|_0$ can be calculated by ray tracing. The phase distribution of the CGH is

$$\phi(x_s, y_s, z_s) = 2\pi \cdot w(x_s, y_s, z_s) / \lambda, \quad (2)$$

where λ is the working wavelength.

Due to the rotational symmetry of the aspheric surfaces, the phase of each point on the same circle of CGH can be obtained as long as that of one point is calculated from Eqs. (1) and (2). Therefore, the phase function can be described as

$$\phi(\rho) = \sum_{i=1}^N \alpha_i \rho^{2i}, \quad (3)$$

where N is the number of polynomial coefficients in series, the coordinate ρ is the radius generalized by the

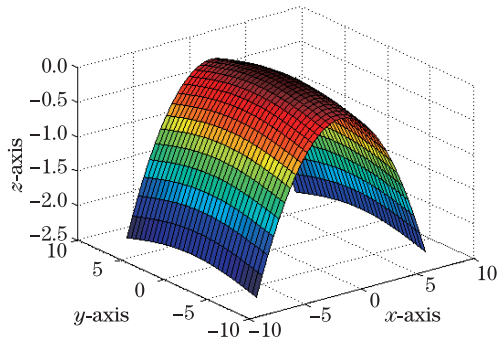


Fig. 3. Freeform surface expressed by Eq. (7).

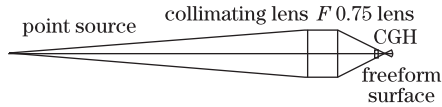


Fig. 4. Null interferometric optical geometry for testing the freeform surface with CGH.

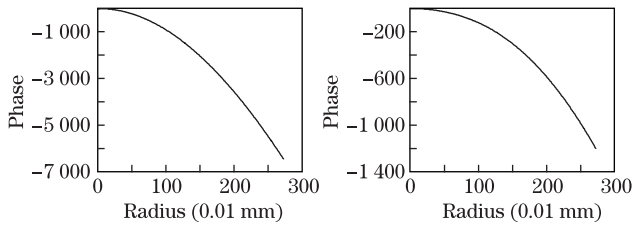


Fig. 5. Phase function plot of the CGH. Phase distribution of CGH of (a) x -axis and (b) y -axis.

coefficients of even terms (including the power of both x and y in Eq. (6)) will be optimized continuously until the value of merit function is smaller than the objective value, because the even terms in the polynomials represent the characteristic of the rotational symmetry which dominates the shape of the tested surface. On the other hand, the coefficients of odd terms representing the characteristic of the non-rotational asymmetry will be optimized continuously until the value of merit function is smaller than the objective value. Then the coefficients of even and odd terms will be optimized in turn until the value of merit function reaches the target. Figure 2 shows the algorithm flow for optimizing the above-mentioned phase polynomials.

For example, using the design method proposed above, a CGH for testing a freeform surface of F - θ lens described as

$$z = ax^2 + by^2 + cy^4, \quad |x| \leq 7.5, |y| \leq 20, \quad (7)$$

where $a = -1/25$, $b = -1/250$, and $c = 1/92000$. The units of x , y , z are millimeters. Figure 3 shows the shape of the freeform surface.

The thickness of the CGH substrate in this example is 5 mm because a thinner CGH substrate is prone to deformation when e-beam lithography is used to make pattern on the substrate and the substrate thickness limit of the e-beam lithography. Figure 4 depicts the null interferometric optical geometry for testing the freeform surface of F - θ lens with CGH. A plane wave is produced by the collimating lens with a point source posited at the focus. After transmitting the $F0.75$ lens, the plane

wave becomes standard sphere. With the departure of the tested surface from the standard sphere compensated by CGH, the wavefront launches onto the tested surface along the corresponding normal direction.

According to Eq. (5), the discrete phase distribution of CGH is calculated. Then the phase function of CGH with inclined carrier frequency for separating diffraction orders is obtained by optimizing the coefficients in Eq. (6) with the algorithm shown in Fig. 2. In this example, the highest power of the phase polynomials is 12 and the number of the coefficients in Eq. (6) is 90. Figure 5 shows the phase function plot of the CGH designed by the new method. Figure 6 depicts wavefront aberration from the CGH. Figure 7 depicts the spot diagram of the autocollimated reflected wave from the freeform surface.

It can be clearly seen from Fig. 5 that the phase increment of the x -axis is faster than that of the y -axis corresponding the gradient change trend of the freeform surface, which means the linewidth of the pattern at x -direction is narrower than that at y -direction. The narrowest linewidth of the pattern on CGH is 700 nm (calculated from Fig. 5), which is a challenge to the fabrication of xxx.

It is observed from Fig. 6 that the peak to valley (PV) value of the wavefront is 0.0065λ and the RMS value is 0.0011λ . The requirements of the design are 0.01λ for PV and 0.001λ for RMS. In Fig. 7, the spot of the wave reflected from the freeform surface to the point source is $0.1 \mu\text{m}$, which means that the wavefront from the CGH launches onto the tested surface along the corresponding normal direction. It can be concluded that the design satisfies the requirements of the null test for the freeform surface.

Figure 8 shows the CGH pattern produced by the L-edit software. The shape of the CGH pattern for testing freeform surfaces is obviously different from that for testing aspheric surfaces. The shape of the CGH pattern for testing aspheric surfaces is circular and the linewidth on the same circular is uniform. However, the shape of the CGH pattern for testing freeform surfaces resembles an ellipse and the linewidth on the same circular is not uniform.

At present, the original procedure of CGH fabricating for testing aspheric surfaces consists six steps, as shown in Fig. 9. The CGH designed above was fabricated following the six-step process. Quartz glass was used as the substrate of CGH. A radio frequency sputtering system (Norodiko NM2000) was used to coat one layer of chrome on the substrate. A Headway R790 spinner was used to spin the photoresist on the chrome. An electron beam lithography system (Crestec CABL-9510C) was used to make pattern. A reactive ion etching system (RIE) (PlasmaTherm 790 system) was used to etch deep step. Figure 10 depicts the CGH fabricated by the six-step procedure.

It is obviously observed from Fig. 10 that the edge of the pattern deformed seriously, indicating that the fabrication of the sample is not successful. Analysis showed that the failures occurred at the third and fourth step in the process where some chemical reagents were used to remove the photoresist and chrome. Due to the uniform linewidth on the same circular of CGH for testing

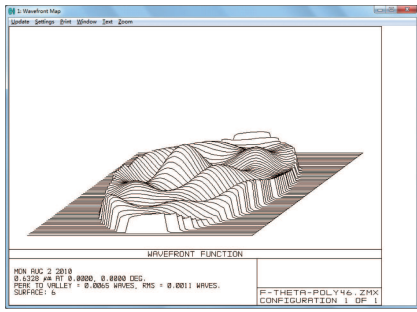


Fig. 6. Wavefront aberration from the CGH.

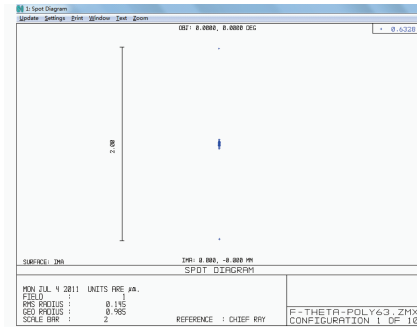


Fig. 7. Spot diagram of reflected wave.

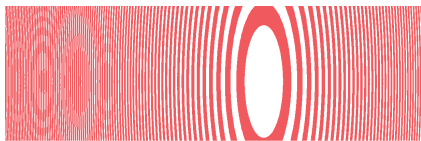


Fig. 8. CGH pattern with L-edit software.

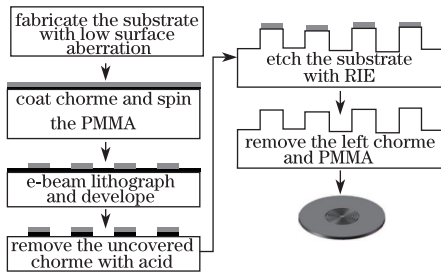


Fig. 9. Six-step procedure for CGH fabricating procedure.



Fig. 10. CGH fabricated by the six-step.

aspheric surfaces, the reaction time of the chemical reagents is the same at different positions of the same circular, which means the phenomenon in Fig. 10 will not occur. However, with the same reaction time, due to the non-uniform linewidth on the same circular of

CGH for testing freeform surfaces, some regions in the same circular reacted incompletely while some regions reacted excessively, leading to the phenomenon in Fig. 10. Figure 11 depicts the pattern after developing in the original procedure. Figure 12 depicts the pattern after removing the uncovered chrome with acid in the original procedure.

In Figs. 11 and 12, deformed edges can be observed because the non-uniform linewidth on the same circular of CGH has not been considered in the original procedure.

After several experiments, a new eight-step fabrication procedure is suggested. At the third step (Fig. 9), the developing time and the concentration of developer are calculated according to the narrowest linewidth of CGH (which indicates some regions react incompletely). Hence, it is proposed to add a new step before the fourth step—using RIE to etch the remain photoresistent in incompletely reacted regions. In the same way, at the fourth step, the time and concentration of acid are calculated according to the narrowest linewidth and a new step—using RIE to etch the remain chrome in incompletely reacted regions—is also suggested. Figure 13 shows the pattern after developing in the new procedure. Figure 14 shows the pattern after removing the uncovered chrome in the new procedure.

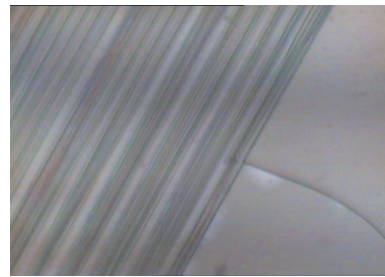


Fig. 11. Pattern after developing in the original procedure.

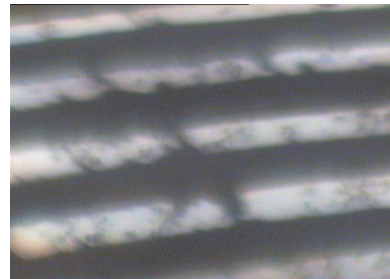


Fig. 12. Pattern after removing chrome in the original procedure.



Fig. 13. Pattern after developing in the new procedure.

It can be observed clearly from Figs. 13 and 14 that the phenomenon in Fig. 10 has not occurred and the edge of the pattern is free of damage. Figure 15 depicts the fabricated CGH with high quality for testing freeform surface of F - θ lens. Figure 16 depicts the test results of the linewidth and depth of CGH pattern by surface profiler (Ambios XP-2). From Fig. 16, the linewidth of the first circular is $24.15 \mu\text{m}$ and the depth of the step is 690 nm , which match the demands of the design ($24\text{-}\mu\text{m}$ linewidth and 692-nm depth).

In conclusion, the non-rotational asymmetry of the freeform surfaces makes the design and fabrication of CGH very difficult. The original rotation design method is invalid in the fabrication of CGH. A novel ray-tracing planning model is proposed to be added into the math model for designing CGH with non-rotational

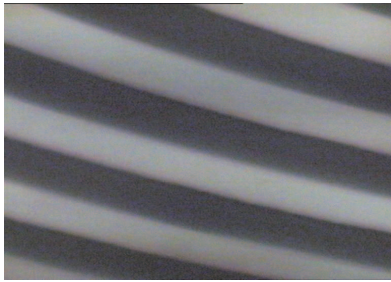


Fig. 14. Pattern after removing chrome in the new procedure.



Fig. 15. CGH fabricated in the new procedure.

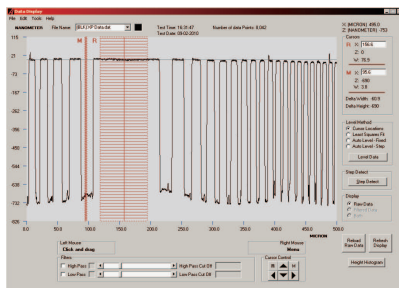


Fig. 16. Test results of surface profiler.

asymmetry. The method of optimizing even and odd power coefficients of phase polynomials in turn is suggested to perform the global optimization. As a result, the CGH whose wavefront aberration is 0.0065λ (PV) and 0.0011λ (RMS) was successfully designed and used in null test for freeform surfaces of F - θ lens. The original six-step fabrication procedure is not proper for non-rotational asymmetry CGH because the non-uniform linewidth on the same circular of CGH has not been considered. A new eight-step fabrication procedure is presented by adding two steps that use RIE to remove the remain photoresistent and chrome in incompletely reacted regions. The results of surface profiler prove that CGH fabricated in the new procedure satisfied the design requirements.

This work was supported by the Natural Science Foundation of Jiangsu Province of China under Grant No. BK2012802.

References

1. A. Arimoto, S. Saitoh, Shigeo Moriyama, Y. Kondou, and T. Mochizuki, *Appl. Opt.* **6**, 699 (1991).
2. W. T. Plummer, J. G. Baker, and J. V. Tassell, *Appl. Opt.* **16**, 3572 (1999).
3. R. B. Li, Z. H. Zhang, X. Du, L. B. Kong, and J. B. Jiang, *Inf. Laser Eng.* (in Chinese) **1**, 110 (2010).
4. R. B. Li, Z. H. Zhang, X. Du, L. B. Kong, and J. B. Jiang, *Jou. Mec. Eng.* (in Chinese) **11**, 137 (2010).
5. E. Garbusi, C. Pruss, J. Liesener, and W. Osten, *Proc. SPIE* **6616**, 661629 (2007).
6. E. Garbusi and W. Osten, *J. Opt. Soc. Am. A* **12**, 2538 (2009).
7. J. H. Burge, C. Zhao, and P. Zhou, *Proc. SPIE* **7739**, 77390T (2010).
8. C. Pruss, S. Reichelt, H. J. Tiziani, and W. Osten, *Opt. Eng.* **11**, 2534 (2004).
9. J. Ma, Z. Gao, R. Zhu, Y. He, L. Chen, J. Li, E. Y. B. Pun, W. H. Wong, L. Huang, C. Xie, X. Zhu, and J. Ma, *Chin. Opt. Lett.* **7**, 70 (2009).
10. H. J. Tiziani, S. Reichelt, C. Pruss, M. Rocktaschel, and U. Hofbauer, *Proc. SPIE* **4440**, 109 (2001).
11. C. Zhao, R. Zehnder, J. H. Burge, and H. M. Martin, *Proc. SPIE* **5869**, 586911 (2005).
12. Z. Gao, M. Kong, R. Zhu, and L. Chen, *Chin. Opt. Lett.* **4**, 241 (2007).
13. Y. Xu, X. Zhang, and Y. Zhang, *Opt. Commun.* **282**, 2327 (2009).
14. P. Su, G. Kang, Q. Tan, and G. Jin, *Chin. Opt. Lett.* **7**, 1097 (2009).
15. P. Su, J. Ma, Q. Tan, G. Kang, Y. Liu, and G. Jin, *Opt. Eng.* **2**, 025801 (2012).